Dissertation submitted to obtain the degree in Master in Science in Biology: Molecular and Cellular Life Sciences

PANCREATIC INTRA-ISLET VESSEL ABLATION AND REGENERATION AS A MODEL FOR PROMOTING ACTIVE BETA AND DELTA CELL CYCLING

STEPHANIE BOURGEOIS

2019-2020

Promotors: Prof. Dr. Nico De Leu; Prof. Dr. Harry Heimberg
Co-promotor: Dr. Willem Staels
Sciences and Bio-engineering Sciences
Beta Cell Neogenesis (BENE), Vrije Universiteit Brussel (VUB)

This Master's thesis came about (in part) during the period in which higher education was subjected to a lockdown and to protective measures to prevent the spread of the COVID-19 virus. Therefore, the process of formatting and data collection, the research method and/or other scientific work involved could not always be carried out in the usual manner. The reader should bear this context in mind when reading this Master's thesis, and also when certain conclusions are being relied upon.

Pancreatic intra-islet vessel ablation and regeneration as a model for promoting active beta and delta cell cycling

Stephanie Bourgeois[1]

[1]*Beta Cell Neogenesis (BENE), Vrije Universiteit Brussel (VUB), Laarbeeklaan 103, 1090 Jette*

Abstract

Background. The shortage in donor beta cells has greatly hindered the widespread use of beta cell transplantation as a therapy for type 1 diabetes (T1D)**.** Regeneration of the endogenous beta cell mass through replication of residual beta cells is currently being envisioned. Pilot experiments from the host lab using a transgenic mouse model that overexpresses sFLT1 by beta cells have demonstrated how recovery from pancreatic intra-islet hypovascularization increases pancreatic endocrine cell cycling *in vivo*.

Aims. The aims of this thesis are to confirm and elaborate aforementioned observations and to evaluate whether the observed increase in pancreatic endocrine cell cycling is a non-specific effect caused by supraphysiological transgene overexpression.

Methods. We used a doxycline-inducible transgenic mouse model in which Vascular Endothelial Growth Factor (VEGF-A) signalling is antagonized within pancreatic islets through beta cell-specific overexpression of a decoy receptor, soluble fms-like tyrosine kinase 1 (sFLT1), leading to islet hypovascularization. Subsequent islet vessel regeneration was induced by withdrawal of doxycyline during which period its effect on active beta and delta cell cycling was analysed.

Results. Active beta cell and delta cycling increased about 2-fold compared to controls. In addition, we obtained preliminary evidence to exclude a role for a non-specific effect caused by supraphysiological transgene overexpression.

Conclusion. Taken together, our intra-islet blood vessel ablation and regeneration model provides an interesting platform to study active beta and delta cell cycling.

Introduction

Type 1 diabetes (T1D) is a chronic metabolic disorder resulting from the autoimmune destruction of pancreatic beta cells. The disease is characterized by the infiltration of pancreatic islets of Langerhans by T-cells and macrophages, resulting in beta cell destruction and, consequently, impaired insulin secretion (Atkinson and Eisenbarth 2001). Since insulin is a key hormone for glucose homeostasis, its deficiency leads to elevated blood glucose levels and subsequent diabetic complications. Although the specific factors triggering this autoimmune attack are not yet fully understood, both genetic and environmental factors are implicated (Noble and Valdes 2011; Rewers and Ludvigsson 2016). T1D patients depend on lifelong exogenous insulin injections which do not represent a real cure since they potentially increase the risk of fatal acute hypoglycaemia and incompletely protect against chronic micro- and macrovascular complications, including nephro/retino/neuropathy, glaucoma, cataract, cerebrovascular disease and coronary and peripheral heart disease (Papatheodorou et al. 2016). All these effects impose a major burden on the physical and psychological quality of life of diabetic patients and culminate in a shortened life expectancy (Huo et al. 2016; Polonsky 1999).

One therapeutic and curative strategy is based on replacement of the beta cell mass by transplantation of islets of Langerhans from donor pancreases. This strategy has already proven its therapeutic value and is clinically applied in a selected group of patients with brittle T1D (Ashoor et al. 2016). However, a major hurdle in this approach is the shortage of donor material. Indeed, multiple donor pancreases are needed to collect sufficient islets for transplantation of one patient (Bottino et al. 2002). Therefore, increasing the endogenous beta cell mass through regeneration would represent an interesting alternative to transplantation and mediate a major progress in the treatment of T1D if combined with strategies that prevent the auto-immune destruction of regenerated beta cells.

Three mechanisms exist by which an organism under normal physiological circumstances is able to increase a specified cell mass: (i) neogenesis (differentiation from stem or precursor cells or transdifferentiation from other mature cell types), (ii) hypertrophy (increased cell size) and (iii) proliferation (increased cell number). Differentiation of beta cells from stem or precursor cells mainly occurs during embryogenesis when PDX1-expressing pancreatic progenitor cells arise in the posterior foregut and expression of the transcription factor NGN3 further commits these cells to an endocrine fate (Murtaugh 2007). Ultimately, a subset of these cells will become pancreatic beta cells. Subsequently, newly-formed beta cells start proliferating, a process that rapidly declines with age (Reers et al. 2009; Scaglia et al. 1997) to reach an extremely low rate of maximum 0.4% in the adult human (Butler et al. 2003, 2010; Perl et al. 2010). The primary mechanism by which postnatal mouse and human beta cells are maintained is by self-duplication rather than differentiation from adult stem or precursor cells (Dor et al. 2004; Georgia and Bhushan 2004; Meier et al. 2008). In case of extreme beta cell depletion, compensatory transdifferentiation of non-beta cells in the endocrine pancreas into insulin-producing cells has been reported (Chera et al. 2014; Thorel et al. 2010). Glucagon-producing alpha cells can convert into beta cells after extensive beta cell ablation, a process that can occur from puberty through adulthood (Thorel et al. 2010). When beta cells were ablated in mice of two weeks old and before weaning, a spontaneous massive reprogramming of somatostatin-producing delta cells

was observed. Additionally, beta cell reconstitution was more efficient and led to diabetes recovery (Chera et al. 2014).

Dissecting the signalling pathways responsible for beta cell mass homeostasis is of great interest for developing novel therapeutic strategies for T1D. Beta cells heavily depend on signals from the islet microenvironment for proper control of their function and mass (Eberhard and Lammert 2009) and are influenced on the level of their gene expression and proliferative capacity by interaction with different other cell types including endocrine, neuronal, immune and endothelial cells and pericytes (Chen et al. 2011; Eberhard and Lammert 2009; Lammert et al. 2001). In this thesis, we are especially interested in the interaction between endocrine and endothelial cells. To allow crosstalk between the peripheral organs and the endocrine pancreas, pancreatic islets are highly vascularized mini-organs in which beta cells are organized in a rosette-like pattern around blood vessels (Geron et al. 2015). This vascularization is essential to supply the islets with nutrients and oxygen and to permit signalling via signalling molecules. Moreover, endothelial cells produce developmental signals for proper early endocrine cell differentiation (Lammert et al. 2001).

A prominent signal by which beta cells and endothelial cells communicate is Vascular Endothelial Growth Factor A (VEGF-A). Beta cells, and, to a lesser extent alpha cells, express and secrete VEGF-A in order to induce angiogenesis (Brissova et al. 2006). VEGF-A binds to its receptor VEGFR2 located on endothelial cells, hereby inducing islet vascularization. Precise control of VEGF-A in adult beta cells is critical for the conservation of a normal beta cell mass and for islet vascular homeostasis. The importance of VEGF-A signalling has been demonstrated in studies of Brissova and collegues. A first study demonstrated that although experimental increase of VEGF-A production in adult mouse beta cells stimulates proliferation of intra-islet endothelial cells, beta cell mass was reduced. Interestingly, 6 weeks after withdrawal of the VEGF-A stimulus, pre-existing beta cells started to proliferate and islet morphology, vascularization, mass and function normalized (Brissova et al. 2014). Inactivation of VEGF-A expression results in a loss of islet vessel density, vessel size and vascular permeability such that the islets have to deal with an impaired oxygen supply (Brissova et al. 2006; D'Hoker et al. 2013). Since oxygen is indispensable for the survival and function of beta cells as well as of many other cell types, organisms have developed tightly regulated pathways to cope with hypoxia (Strowitzki et al. 2019). This capacity to adapt to hypoxia is mediated through the activation of the hypoxia inducible factor (HIF) pathway. HIFs are made up of two subunits: HIF-α and HIF-β. When non-mitochondrial oxygen is sufficiently available (normoxia), HIF-α is hydroxylated by HIF-prolyl hydroxylases (PHDs) and by the factor inhibiting HIF (FIH). Consequently HIF-α will be destabilized by ubiquitination via the von-Hippel Lindau pathway and degraded by proteasomes. However, under hypoxic conditions, hydroxylation of HIF-α subunits is lower, and consequently, these subunits will accumulate. HIF-α will then form a complex with HIF-β, move to the nucleus and induce the transcription of HIF-target genes which generate an adaptive response to hypoxia (Strowitzki et al. 2019). One of the target genes includes VEGF-A, as described above, a major pro-angiogenic factor secreted by both alpha and beta cells. D'Hoker et al. reported that beta cells have a remarkable capacity to cope with intra-islet hypoxia. Hypoxia only moderately affected blood glucose tolerance, while beta cell mass and proliferation remained unaffected (D'Hoker et al. 2013).

The hypoxic state of the islets of Langerhans was created by using a transgenic RIP-rtTA;tetO-sFLT1 mouse model (D'Hoker et al. 2013) in which a reverse tetracycline *trans*-activator (rtTA) is placed under control of a rat insulin gene promotor (RIP). When doxycycline (DOX) is administered via the drinking water, rtTA binds to the operator sequence (TetO) of *sFLT1,* thereby activating the transcription of the soluble VEGF receptor sFLT1. sFLT is a splice-variant of the VEGF receptor 1 (FLT1) that antagonizes VEGF-A signalling by trapping endogenous VEGF-A (**Figure 1a**). DOX was given for 14 days and then stopped to start the withdrawal (WD) phase (**Figure 1b**). Pioneering work by the BENE research group showed that after a period of islet hypoxia, endocrine cells in the pancreatic islets activate their cell cycle at a supraphysiological rate (Staels et al., unpublished) (**Figure 1 c and d**). These results, however, need further elaboration and confirmation. Here, we aim to further investigate the effects of VEGF-A signalling interference and recovery on the islet microenvironment. Together these data could provide insight in the design of a novel strategy to increase the available beta cells mass, an obvious priority in diabetes research.

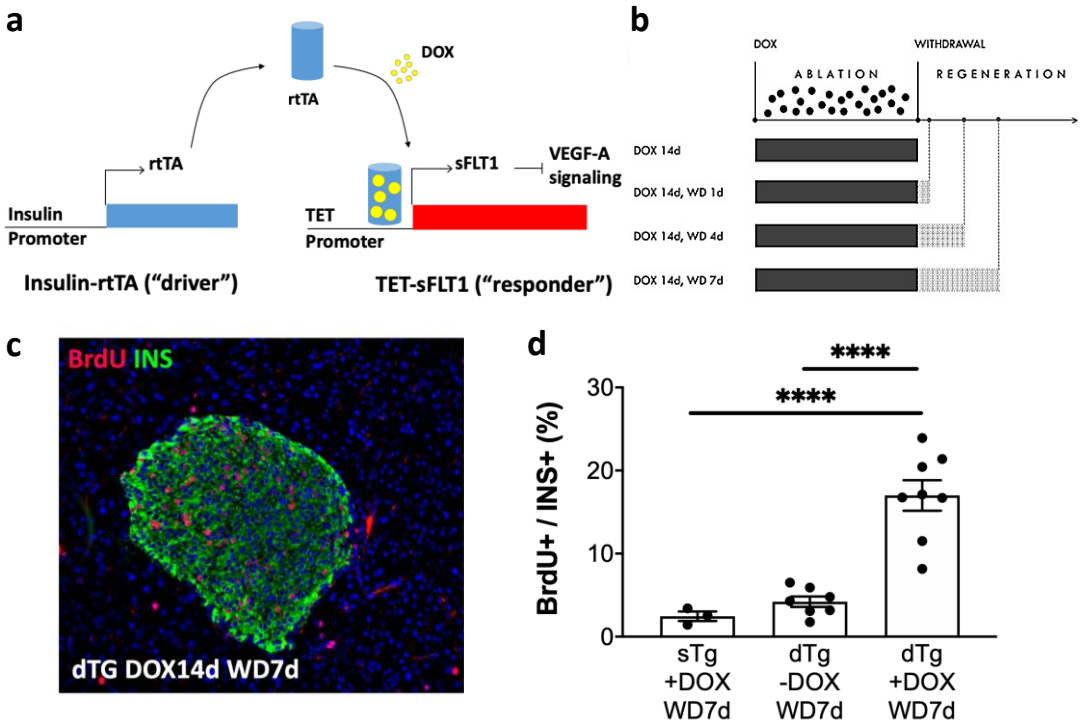

Figure 1| Pancreatic islet vessel ablation regeneration and regeneration promotes endocrine cell cycling. (a) RIP-rtTA;tetO-sFLT1 mice express rtTA under control of a rat insulin promotor (RIP). The DNA-binding activity of the transcription factor rtTA is induced by doxycycline (DOX), which is administered to the mice through their drinking water. Binding of rtTA to the TET-operator induces expression of the soluble receptor sFLT1 that antagonizes VEGF-A signalling by trapping endogenous VEGF-A and causes islet hypovascularization. **(b)** DOX was administered to the mice for 14 days, followed by its withdrawal during 1, 4 or 7 days. **(c)** Immunostaining for BrdU, INS and DNA on pancreatic tissue of a dTg mouse that received DOX for 14 days, followed by 7 days of withdrawal. **(d)** Quantification of the percentage of BrdU+ cells within the insulin positive area in sTg 14d +DOX WD7d, dTg no DOX WD7d and dTg +DOX WD7d mice revealed that active endocrine cell cycling in dTg +DOX WD7d mice was significantly increased. Data were analysed by One-way ANOVA and are represented as mean ± SEM. ****$p \leq 0.0001$

Results

sFLT1 expression by beta cells reduces the islet vascular network

Following vessel ablation by inhibition of VEGF-A signalling near beta cells, and subsequent hypoxia in the islets of Langerhans, pancreatic endocrine cell clusters activate their cell cycle at a supra-physiological rate (Staels and colleagues, unpublished). To confirm and further dissect these data, we conditionally ablated the pancreatic islet blood vessels of double transgenic (dTg) RIP-rtTA;tetO-sFLT1 mice followed by a reinstatement of VEGF-A signalling and, subsequent blood vessel regeneration (a.k.a. "withdrawal" period). We administered doxycyline (DOX) for two weeks through the drinking water, followed by either 1 , 4 or 7 days DOX withdrawal (WD). As a control sTg +DOX or dTg mice that did not receive DOX (no DOX) were used. During the WD period, BrdU was administered continuously to evaluate S-phase activity within cycling cells. To validate the model, immunostaining for insulin and sFLT1 was performed on pancreas sections and the percentage of sFLT1 expressing beta cells was quantified using Fiji image analysis software. sFLT1 was efficiently expressed in the islets of dTg +DOX mice compared to the dTg no DOX mice and its expression decreased in a time-dependent manner during the WD period (**Figure 2a**), starting from 42.6 ± 0.9 % in DOX 14d WD 1d (n = 3) and further decreasing to 34.6 ± 6.5 % in DOX 14d WD 4d (n = 2) and 19.8 ± 2.0 % in DOX 14d WD 7d (n = 9) (**Figure 2b, Supplementary table S1**). We noticed the presence of some basal leakage of sFLT1 (2.7 ± 0.7%) in the dTg mice that did not receive DOX (n = 4).

To evaluate islet vascularization, mice were injected intravenously with tomato-lectin at endpoint. Tomato-lectin can be used as an effective functional blood vessel marker as it binds to glycoconjugates concentrated in the glycocalyx and in the basal membrane of endothelial cells (Mazzetti et al. 2004). Vascularization was significantly lower in the islets of DOX-administered mice compared to the islets of control dTg no DOX mice (**Figure 2c and d, Supplementary table S2**); 7.8 ± 0.7 % in dTg no DOX (n = 5); 1.7 ± 0.1 % in DOX 14d WD 1d (n = 3); 1.4 ± 0.1 % in DOX 14d WD 4d (n = 2) and 2.3 ± 0.2 % in DOX 14d WD 7d (n=8). Taken together, these data show that beta cell-specific sFLT1 expression severely reduced the islet vascular network and that vessel density did not significantly recover up to 7 days after DOX WD (**Supplementary table S2**).

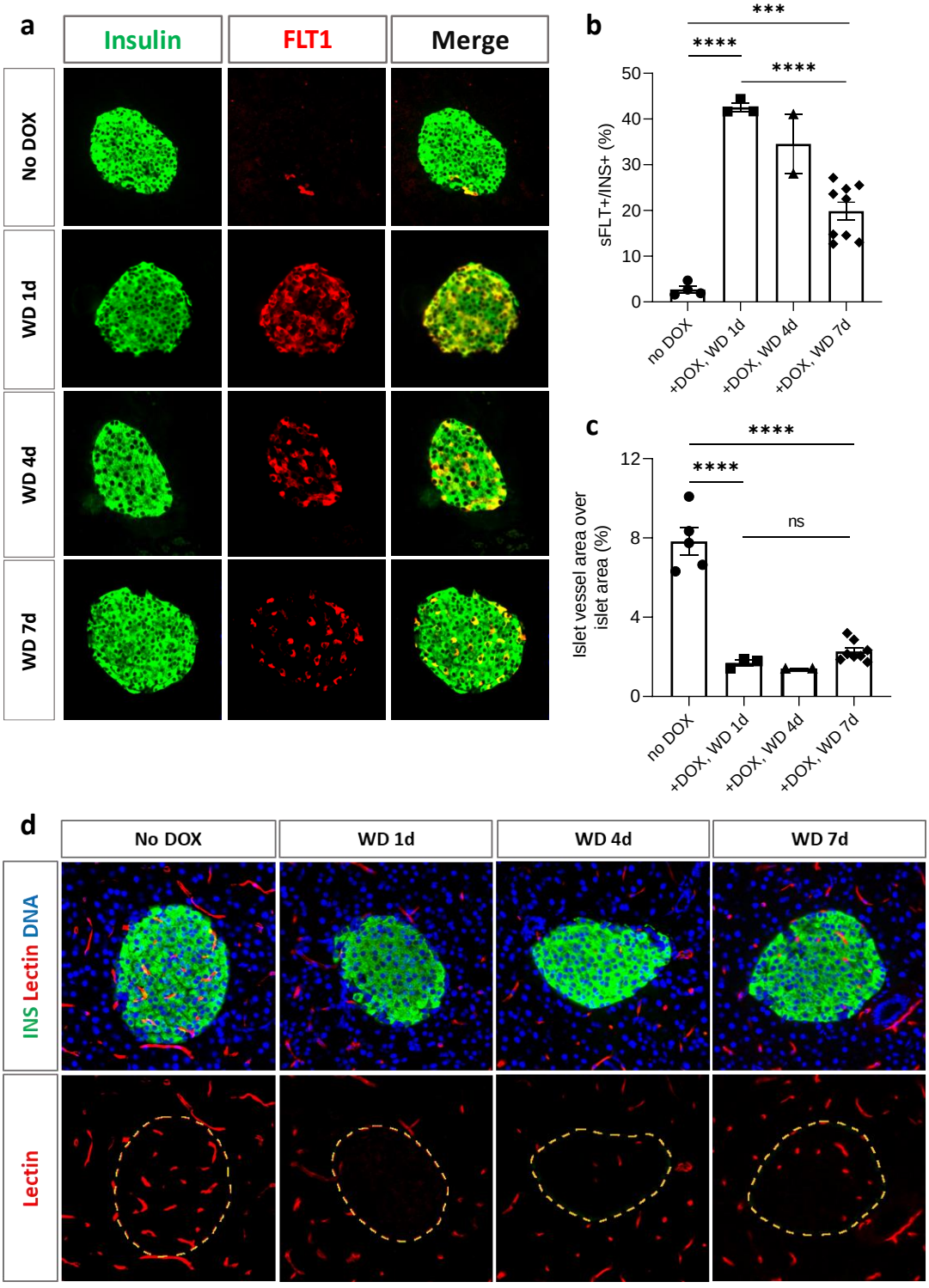

Figure 2 | sFLT1 expression by beta cells reduces the islet vascular network. (a) Immunostaining on pancreas sections for insulin (green) and sFLT1 (red) from dTg no DOX and dTg DOX 14d WD 1d, 4d and 7d mice. **(b)** sFLT1 is efficiently expressed in the pancreatic islets of dTg DOX 14d WD 1, 4, 7d mice compared to the dTg no DOX control mice and its expression decreases in a time-dependent manner after DOX WD (no DOX vs +DOX WD 1d, $p < 0.0001$; no DOX vs +DOX WD 7d, $p = 0.0001$ and +DOX WD 1d vs +DOX WD 7d, $p < 0.0001$). **(c)** sFLT1 expression significantly reduces the islet vascular network. Vessel density is calculated as the proportion of tomato lectin-positive vessels per islet area (no DOX vs +DOX WD 1d, $p < 0.0001$; no DOX vs +DOX WD 7d, $p < 0.0001$ and +DOX WD 1d vs +DOX WD 7d, ns). **(d)** Immunostaining on pancreas sections for insulin (green) and tomato lectin (red) of dTg no DOX and dTg DOX 14d WD 1d, 4d and 7d mice. DNA is stained blue (Hoechst). Data were analysed by a One-way ANOVA and are represented as mean ± SEM. ***$p \leq 0.001$. ****$p \leq 0.0001$

Islet hypovascularization and hypoxia impairs fasting blood glucose

To examine the effect of islet vessel ablation and regeneration on blood glucose homeostasis, two hours fasting glycaemia was measured weekly in dTg no DOX, sTg DOX 14d WD 1d, 4d, 7d and dTg DOX 14d WD 1d, 4d and 7d mice. During DOX administration, blood glucose levels of dTg mice increased significantly, from an average of 160.6 ± 7.7 mg/dL (n=20) on day 0 (before start of DOX administration), to an average of 198.2 ± 9.5 mg/dL on day 14 (end of DOX administration) (p = 0.009) (**Figure 3a-d, Supplementary table S3**). Compared to the control sTg +DOX 14d, fasting glycaemia was significantly higher after two weeks of DOX administration (p = 0.0007), but not if compared to dTg no DOX mice. Blood glucose values were 165.3 ± 18.7 mg/dL in dTg no DOX mice (n=8), 143.2 ± 7.1 mg/dL in sTg +DOX 14d (n=15) and 198.2 ± 9.5 mg/dL dTg DOX 14d (n=20) (**Supplementary table S6**). Blood glucose levels gradually decreased over the course of the WD period to an average of 137.8 ± 5.0 mg/dL in dTg no DOX WD 7d mice (n=8), 137.1 ± 3.6 mg/dL in sTg +DOX 14d WD 7d (n=11) and 155.6 ± 5.2 mg/dL dTg DOX 14d WD 7d mice (n=14) (**Figure 3e, Supplementary table S7**).

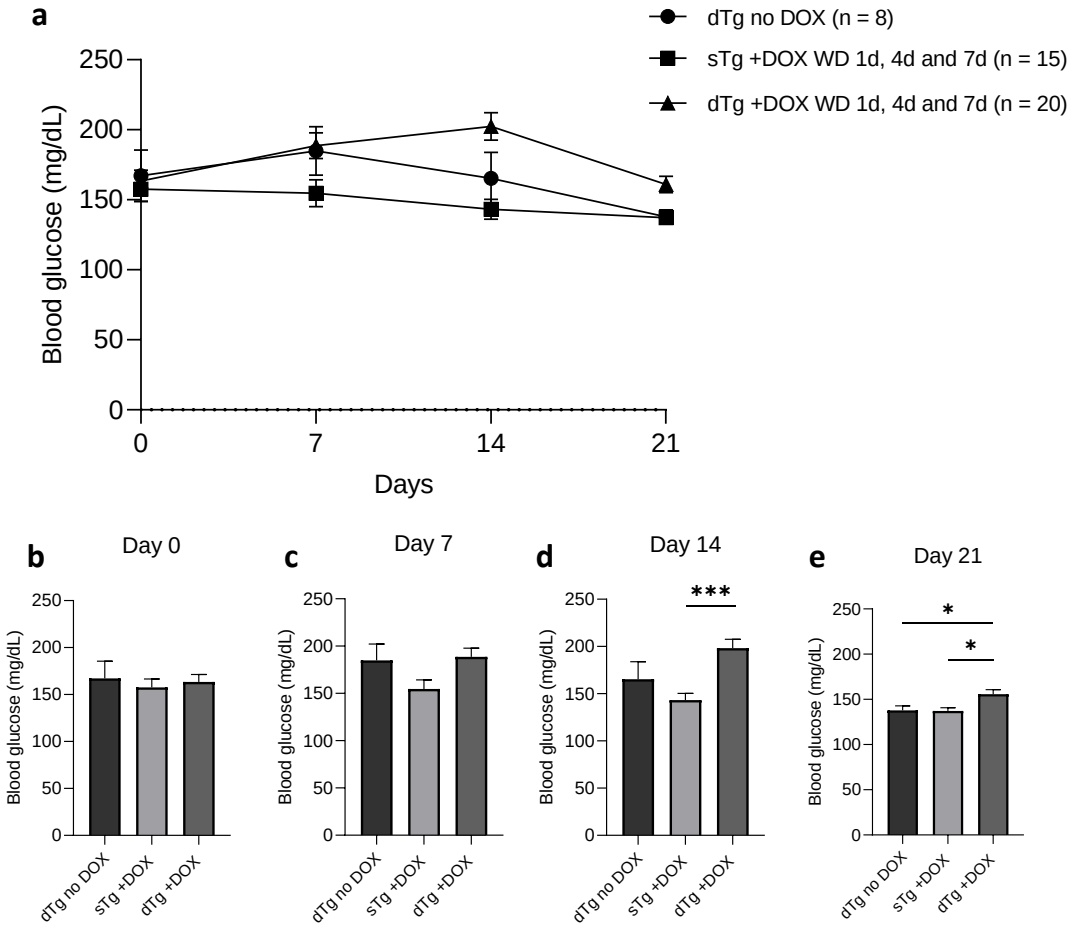

Figure 3 | Islet hypovascularization and hypoxia impairs fasting blood glucose. (a) 2hrs fasting glycaemia of dTg no DOX, sTg DOX 14d WD 1d, 4d, 7d and dTg DOX 14d WD 1d, 4d, 7d mice. **(b)** 2hrs fasting glycaemia at day 0 (before start of DOX administration) (No significant difference in blood glucose values between any of the groups.) **(c)** 2hrs fasting glycaemia at day 7 of DOX administration. (No significant difference in blood glucose values between any of the groups.) **(d)** 2hrs fasting glycaemia at day 14 of DOX administration. (dTg no DOX vs sTg no DOX, ns; dTg no DOX vs dTg +DOX, ns; sTg +DOX vs dTg +DOX, p = 0.0007). **(E)** 2hrs fasting glycaemia at 7 days withdrawal of DOX administration (Day 21) (dTg no DOX vs sTg no DOX, ns; dTg no DOX vs dTg +DOX, p = 0.0437; sTg +DOX vs dTg +DOX, p = 0.0192). Data were analysed by one-way ANOVA and are represented as mean ± SEM. *p ≤ 0.05, ***p ≤ 0.001

Recovery from intra-islet hypovascularization and hypoxia promotes active beta cell cycling

Previously, Staels and colleagues reported that after a transient period of islet hypovascularization and hypoxia, beta cells activate their cell cycle at a supra-physiological rate. Consistent with this finding, active beta cell cycling was indeed significantly increased in dTg DOX 14d WD 7d compared to dTg WD 7d no DOX and sTg +DOX WD7D mice (**Figure 4a and b, Supplementary table S8**). 7 days of cumulative BrdU labelling revealed that 2.7 ± 0.3 % of beta cells were actively cycling in dTg no DOX WD 7d mice (n = 8), 3.5 ± 0.6 in sTg +DOX WD 7d (n = 6) mice as compared to 6.5 ± 0.7 % in dTg DOX 14d WD 7d (n = 10) (**Figure 4b, Supplementary table S8**). Resulting in a mean fold change of 2.4 ± 0.3 in active beta cell cycling (normalized against dTg no DOX WD 7d mice) (**Figure 4c, Supplementary table S9**). Taken together, these data indicate that recovery from intra-islet vessel ablation promotes active beta cell cycling.

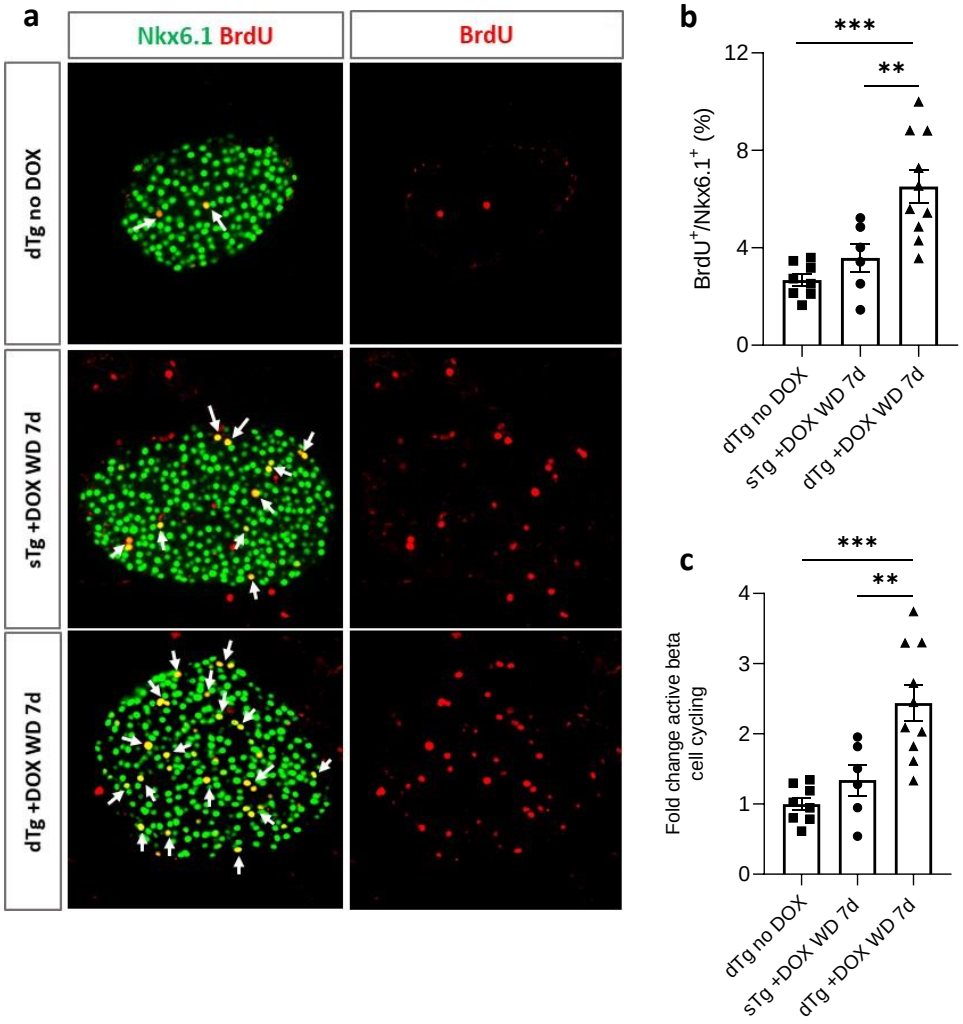

Figure 4 | Recovery from intra-islet hypovascularization and hypoxia promotes active beta cell cycling. (a) Pancreas tissue sections were stained for NKX6.1 (green) and BrdU (red) to analyze active beta cell cycling. Cycling beta cells are indicated with arrows. **(b)** Quantification of active beta cell cycling. (dTg no DOX vs sTg +DOX WD 7d, ns; dTg no DOX vs dTg +DOX WD 7d, p = 0.0002; sTg +DOX WD 7d vs dTg +DOX WD 7d, p = 0.0058). **(c)** Active beta cell cycling increased 2.4 ± 0.25 fold in dTg DOX 14d WD 7d compared to dTg no DOX mice (dTg no DOX vs sTg +DOX WD 7d, ns; dTg no DOX vs dTg +DOX WD 7d, p = 0.0002; sTg +DOX WD 7d vs dTg +DOX WD 7d, p = 0.0058) . Data were analysed by One-way ANOVA and are represented as mean ± SEM. ** ≤ 0.01, ***p ≤ 0.001.

Recovery from intra-islet hypovascularization and hypoxia promotes active delta cell cycling

To further investigate the effect of recovery from intra-islet hypovascularization and hypoxia on endocrine cell proliferation, active delta cell cycling was measured in dTg no DOX, sTg +DOX WD 7d and dTg +DOX WD 7d mice. 7 days of cumulative BrdU labelling revealed that active delta cell cycling was significantly increased with 6.4 ± 0.5 % (n=14) in dTg +DOX WD7D mice compared to 3.3 ± 2.2 % (n=6) in dTg no DOX mice and also to 3.5 ± 0.4 % (n = 8) in sTg +DOX WD7D (**Figure 5a and b, Supplementary table S10**). This resulted in a mean fold change of 1.9 ± 0.2 (normalized against dTg no DOX WD 7d mice) (**Figure 5c, Supplementary table S11**). These data reveal that not only active beta cell cycling is promoted after intra-islet vessel ablation, but also active delta cell cycling and hereby confirm the observations of Staels et al.

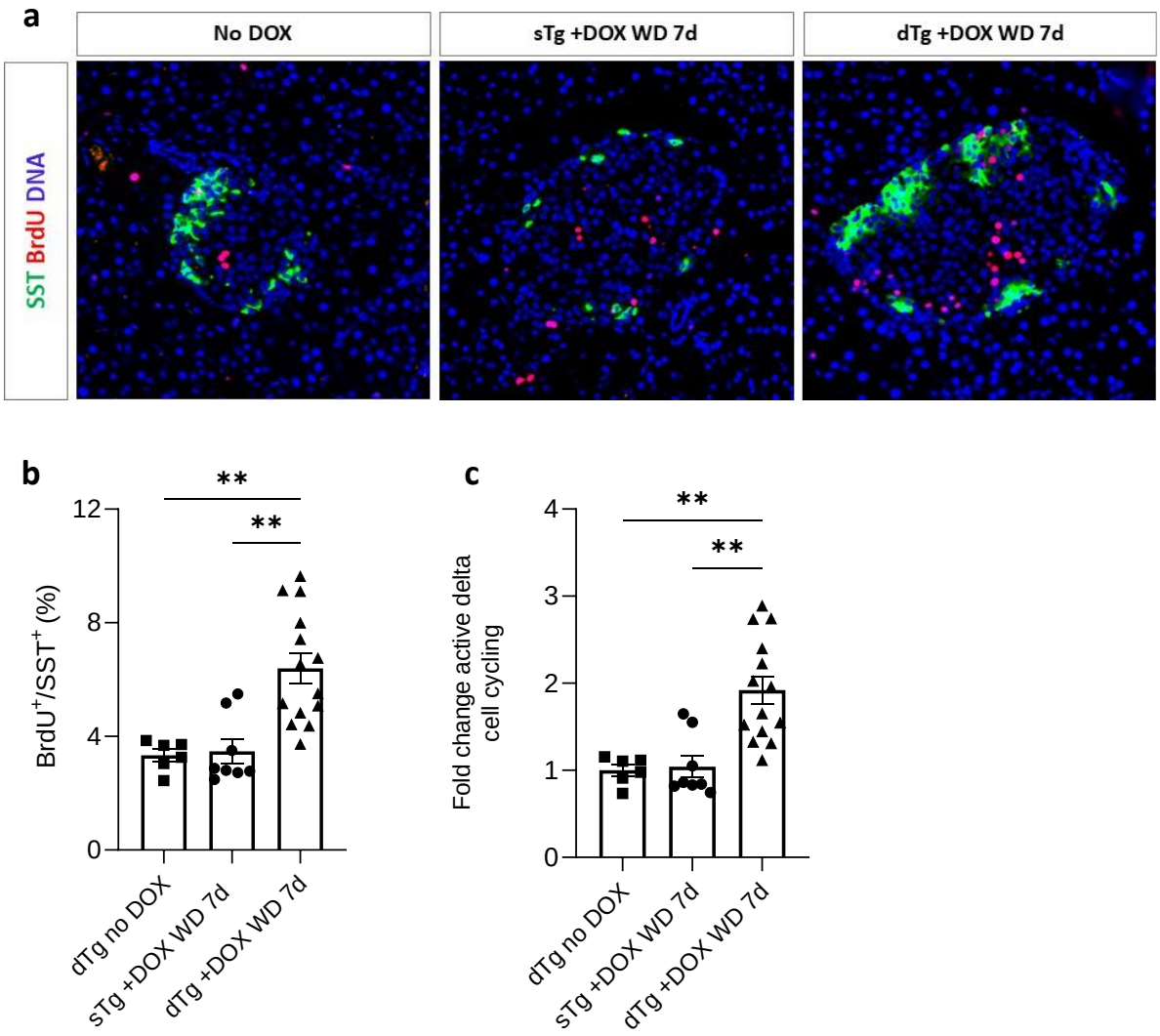

Figure 5 | Recovery from intra-islet hypovascularization and hypoxia promotes active delta cell cycling. (a) Pancreas tissue sections were stained for Somatostatin (green) and BrdU (red). DNA is stained blue (Hoechst). **(b)** Quantification of active delta cell cycling. (dTg no DOX vs sTg +DOX WD 7d, ns; dTg no DOX vs dTg +DOX WD 7d, p = 0.0069; sTg +DOX WD 7d vs dTg +DOX WD 7d, p = 0.0028). **(c)** Active delta cycling cycling increased 1.9 ± 0.16 fold in dTg +DOX WD 7d and 1.0 ± 0.13 in sTg +DOX WD 7d, values were normalized against dTg no DOX WD 7d. (dTg no DOX vs sTg +DOX WD 7d, ns; dTg no DOX vs dTg +DOX WD 7d, p = 0.0069; sTg +DOX WD 7d vs dTg +DOX WD 7d, p = 0.0028). Data were analysed by a One-way ANOVA using the Kruskal-Wallis test and are represented as mean ± SEM. ** p ≤ 0.01.

The increase in active beta cell cycling is transgene-specific

To exclude the possibility that the increase in active beta cell cycling may be a non-specific effect induced by supra-physiological overexpression of a transgene, RIP-rtTA;TetO-GFP mice were used as a control transgenic mouse model that expresses Green Fluorescent Protein (GFP) instead of sFLT1 under control of the RIP promoter upon DOX administration (**Figure 6a**). Subsequently, these mice will not develop hypovascular and hypoxic islets. In parallel with our previous experiments, DOX was administered to the mice for 14 days through their drinking water followed by a seven days withdrawal period with continuous BrdU administration.

To hours fasting glycaemia was measured weekly. Expression of GFP did not impair blood glucose homeostasis (**Figure 6b, Supplementary table S12**) and no significant difference in fasting glycaemia was observed between DOX-administered mice and the control group (**Figure 6b, Supplementary table S13**). As expected, GFP expression decreased in a time-dependent manner during the withdrawal period, from 29.6 ± 1.6 % in dTg DOX 14d (n=3) to 14.9 ± 2.1 % in dTg DOX 14d W D 7d (n=5) (**Figure 6c and d, Supplementary table S14**). In control dTg no DOX mice, GFP expression was either completely absent or detected in a very low number of cells and was therefore not quantified. Active beta cell cycling was 7.3 ± 0.6 % in dTg +DOX WD7D mice (n=9) compared to 4.7 ± 1.3 % in dTg no DOX mice (n=5) (Not statistically significant) (**Figure 6f, Supplementary table S15**). In conclusion, no significant increase in active beta cell cycling was observed between the dTg DOX 14d WD 7d mice and the dTg no DOX control mice.

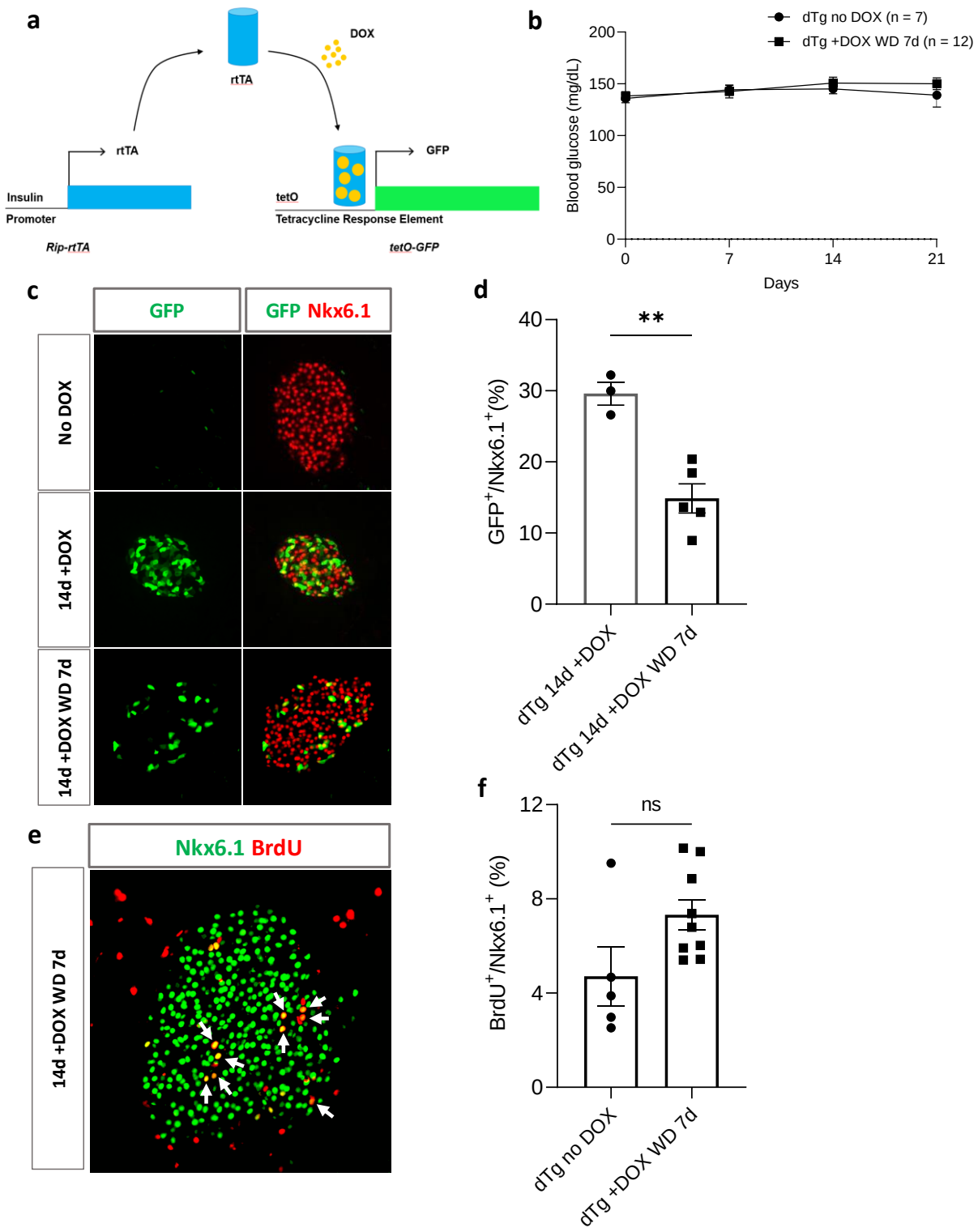

Figure 6 | RIP-rtTA;TetO-GFP double transgenic mouse model. (a) Schematic representation of the dTg control mouse model: RIP-rtTA;tetO-GFP mice express rtTA under control of a rat insulin promotor (RIP). The DNA-binding activity of the transcription factor rtTA is induced by doxycycline (DOX), which is provided to the mice through their drinking water. Binding of rtTA to the TET-operator induces expression of Green Fluorescent Protein (GFP). **(b)** 2hrs fasting glycaemia of dTg no DOX and dTg +DOX 14d WD 7d mice. (There was no significant difference in blood glucose values between any of the groups.) **(C)** Immunostaining on pancreas sections for GFP (green) and NKX6.1 (red). **(d)** Quantification of GFP-expressing beta cells in dTg DOX 14d and dTg DOX 14d WD 7d mice. ($p = 0.0026$). **(e)** Pancreas tissue sections were stained for NKX6.1 (green) and BrdU (red) to analyze active beta cell cycling. Cycling beta cells are indicated with arrows. **(f)** Quantification of active beta cell cycling. ($p = 0.0588$, ns). Data were analysed by an unpaired t-test and are represented as mean ± SEM.** $p \leq 0.01$.

Discussion

Although beta cell transplantation has proven its therapeutic value for patients with brittle type 1 diabetes, the shortage of donor beta cells and their substantial loss following transplantation has greatly hindered its widespread clinical use (Ashoor et al. 2016; Ryan et al. 2002). Finding strategies to increase the available beta cell mass for transplantation could greatly benefit islet transplantation programs. Extensive knowledge on the beta cell-microenvironment and signalling between beta cells and other cell types is required to understand the kinetics of and mechanisms driving beta cell proliferation. Over the last decade, our research group has extensively studied the interaction between pancreatic beta cells and endothelial cells. To this purpose, a transgenic mouse model of conditional islet hypovascularization and hypoxia through inhibition of VEGF-A signalling has been created (D'Hoker et al. 2013). Notably, using this model, Staels and colleagues observed that after a period of islet vessel ablation, active beta cell cycling was increased and gave rise to an enlarged beta cell mass (unpublished data). These findings, however, needed further confirmation and elaboration. We therefore used the same double transgenic (dTg) RIP-rtTA;tetO-sFLT1 mouse model to induce doxycycline (DOX)-mediated conditional islet blood vessel ablation and regeneration.

We found that sFLT1 was successfully expressed in the islets of dTg +DOX mice and that its expression decreased in a time-dependent manner upon DOX withdrawal (WD). Scavenging endogenous VEGF-A near the pancreatic beta cells, through transgenic overexpression of its soluble FLT1 receptor by beta cells, led to a rapid and drastic regression of the intra-islet vascular network. These findings are in line with a previous study by Brissova et al., in which VEGF-A expression by pancreatic beta cells was inhibited using a Cre-LoxP system that reduced VEGF-A expression by beta cells with 70%, resulting in fewer intra-islet blood vessels compared to wild-type islets but also to a reduced size and branching of the remaining vessels without impacting islet morphology nor beta cell mass (Brissova et al. 2006).

In our experimental model, islet hypovascularization significantly increased the fasting blood glucose levels which is in line with previous studies from our lab (D'Hoker et al. 2013; Staels et al. 2017). Notably, we observed that during one of the experiments the fasting blood glucose values increased to a level that was considerably higher than in the other experiments. Including the values of this experiment increased the average fasting glycaemia at 2 weeks of DOX administration from 179.6 ± 7.5 mg/dL to 198.2 ± 9.5 mg/dL. During this experiment, construction works with accompanying vibrations and noise disturbances were ongoing in the animalarium that were likely stressful for the mice and may have caused the aberrant measurements. If these aberrantly elevated glycaemia values are excluded, fasting glycaemia of the dTg +DOX group is significantly higher compared to the dTg no DOX group ($p < 0.001$) as well as to the sTg +DOX group ($p < 0.0001$) at 2 weeks of DOX administration. As isolated hypovascularized islets are not functionally impaired (D'Hoker et al. 2013; Staels et al. 2017), the observed increase in blood glucose levels during DOX administration in our model likely results from impaired glucose sensing and insulin release caused by hypovascularization of the islets of Langerhans rather than by overt beta cell dysfunction. Indeed, adult islets are highly vascularized mini-organs that highly depend on extensive vascularization for proper blood glucose sensing and fast insulin secretion (Lammert et al. 2003; Lammert et al. 2001; Nikolova et al. 2006). Although the islets

were not completely revascularized, blood glucose levels tended to normalize at the end of the DOX withdrawal period.

We hypothesize that the increased active beta and delta cell cycling that was observed upon islet vessel regeneration may be a consequence of the restoration of the endocrine-endothelial cell cross-talk. During the DOX treatment period, the reciprocal paracrine signalling between endocrine and endothelial cells will be impaired if VEGF-A is scavenged by sFLT1. Endothelial cells produce essential molecules for beta cells, such as tissue Growth Factor (CTGF) for example, that upregulates positive cell-cycle regulators and factors involved in beta cell proliferation (Guney et al. 2011; Riley et al. 2015). We suggest that when sFLT1 overexpression ends, the subsequent release of VEGF-A molecules activates the endothelial cells and resumes paracrine signalling. This may induce an activation of the endocrine cell cycle.

Alternatively, the abovementioned transient period of hyperglycaemia may have been a trigger for beta cell proliferation. A study by Alonso et al. reported that a moderate sustained increase in glycemia in mice resulted in a compensatory increase in beta cell proliferation, occurring with a delay of several days (Alonso et al. 2007). However, the same phenomenon has not yet been reported in delta cells. Interestingly, Szabat et al. provided evidence that the increase in beta cell proliferation was not necessarily a consequence of the hyperglycaemia itself, but rather of the reduced insulin production by the beta cells. In case of normal physiological insulin secretion, the associated sub-threshold chronic endoplasmic reticulum (ER) stress suppresses beta cell proliferation. Lowering this burden by removal of the insulin gene relieves baseline ER stress and promotes beta cell replication (Szabat et al. 2016). In order to exclude the possibility that hyperglycaemia triggers beta (and delta) cell replication in our model, we envision to maintain normoglycaemia during DOX administration through exogenous insulin administration or islet cell transplantation.

Notably, active beta cell cycling as observed in this study was in general lower than previously detected by Staels and colleagues. We noticed that the number of beta cells that still produced sFLT1 in the DOX withdrawal period was lower as compared to the values previously observed by Staels et al. and, additionally, there seemed to be some basal leakiness of sFLT1 expression, i.e. production of sFLT1 in the absence of DOX. Since we hypothesize that a sudden increase of VEGF-A signalling after a period of inhibition initiates a boost in cell cycling, a lower expression of sFLT1 during the DOX treatment period might cause a smaller sudden release of VEGF-A in the DOX withdrawal period, resulting in a smaller boost in cell cycling. Moreover, the presence of transgene leakiness may have also dampened the sudden restoration of VEGF-A signalling. Transgene leakiness in TetO/TetOff technologies has already been described in previous studies (Lewandoski 2001; Ryding et al. 2001).

We used RIP-rtTA;tetO-GFP mice which overexpress GFP (dTg^{GFP}) instead of sFLT1 to exclude the possibility that the observed increase in active beta cell cycling was not related to overexpression of sFLT1 *per se* but rather to a compensatory response after a transient period of beta cell stress provoked by transgene overexpression. Although literature on this topic is sparse, some studies suggest that this may be possible. It has been reported that over-expression of transgenes in mouse lense can induce endoplasmic reticulum (ER) stress and activate unfolded protein response (UPR) signalling pathways (Reneker et al. 2011). Remarkably, the beta cell UPR has been described as a regulator of beta cell

replication through its ability to sense insulin production. Beta cells with an active UPR, are more likely to replicate (Sharma et al. 2015).

We observed that active beta cell cycling was not significantly increased in dTg^{GFP} +DOX WD 7d mice compared to dTg^{GFP} no DOX. This observation, however, warrants further investigation as a large standard deviation was observed in the dTg^{GFP} no DOX control group and as only two independent experiments were carried out. Noteworthy, it should be considered that, in contrast to sFLT1, GFP is not secreted by the beta cells (Roh et al. 2013) and has a relatively long half-life (Corish and Tyler-Smith 1999). Consequently, compared to sFLT1, there may be more GFP protein per cell which could cause relatively more cellular stress and relatively more active beta cell cycling upon its relief. Immunoblot analysis of isolated beta cells from both transgenic strains after DOX administration could be used to measure the relative amount of GFP or sFLT1 protein per cell. An ideal transgenic mouse model to test this hypothesis would be one that expresses a variant of sFLT1 that is not able to bind VEGF-A. Nevertheless, supra-physiological transgene overexpression cannot explain the observed increase in active delta cell cycling since the transgene, whether it be sFLT1 or GFP, is overexpressed only by beta cells.

Since the number of repeats was limited under some experimental conditions, the obtained means and standard errors might differ significantly from the true values. This limitation should be taken into account when interpreting our data. Furthermore, the quantification of sFLT1 and GFP expression, vessel area, and active beta and delta cell cycling was performed through analysis of immunofluorescent staining. The heterogeneity in expression and degradation of proteins, the quality of the staining, the presence of autofluorescence and the varying uptake of BrdU in cells (Bonhoeffer et al. 2020) can be reflected in different staining intensities. This implies the presence of a marginal error which, however, should not influence the overall conclusions. As a follow-up of this study we intend to explore the mechanism that underlies the observed increase in active beta (and delta) cell cycling by single-cell RNA sequencing (Grün et al. 2016; Muraro et al. 2016) of beta (and delta) cells isolated at the peak of proliferation.

In conclusion, the intra-Islet vessel ablation and regeneration model provides an interesting platform for studying active beta and delta cell cycling. Insights obtained from this model may inspire the development of novel strategies to promote beta cell (re)generation to alleviate the pressure on the already scarce pool of donor beta cells.

Acknowledgements

I would like to thank my thesis promotors and co-promotor Prof. Dr. Nico De Leu, Prof. Dr. Harry Heimberg and Dr. Willem Staels for their constant feedback and guidance. I'm also very grateful for the practical support and assistance of Dr. Yves Heremans. Furthermore, I would like to thank Gunter Leuckx, Silke Smeets, Yannick Verdonck, Ann Demarré and Veerle Laurysens for their helpful attitude and making it a pleasant and supportive work environment.

Materials and Methods

Animal procedures

All animal experiments were conducted in accordance with the guidelines of the VUB ethical committee for animal experiments and with national guidelines. Mice were housed in individually ventilated cages with up to four littermates per cage, maintained under a 14/10 light-dark cycle and fed a standard rodent diet and water ad libitum. Genotyping was performed on tail snips (see below). 6-8 week old RIP-rtTA;TetO-sFLT1 double transgenic (dTG), TetO-sFLT1 single transgenic (sTG) and RIP-rtTA;TetO-GFP mice were randomly assigned to either the doxycycline (DOX)-receiving group or to the control group (no DOX) and further randomized into the withdrawal (WD) 1d, WD 4d or WD 7d endpoint groups prior to any experimental procedures. Drinking water containing DOX (0.4 mg/mL doxycycline hyclate, Sigma-Aldrich, St. Louis, MO, USA) was acidified to pH 3.0 and sweetened with Canderel. Drinking water containing BrdU (0.8 mg/mL, Sigma-Aldrich) was sweetened similarly. Drinking water was changed twice weekly. Body weight and tail vein blood glucose levels were measured weekly using a standard blood glucometer (Glucocard X-meter, Arkray, Kyoto, Japan) after 2 hours of fasting.

Before sacrifice, mice were put under a heat lamp for 10 min., followed by an intravenous tail injection with biotinylated tomato lectin (200 uL 2 mg/mL, Lycopersicon esculentum, Vector Laboratories, Burlingame, CA, USA). Mice were anesthetized by intraperitoneal injection of 100 mg/kg ketamine and 10 mg/kg xylazine. Blood cells were flushed from the circulation of anesthetized mice via cardiac puncture and systemic perfusion with phosphate-buffered saline (PBS). The pancreas and spleen were removed and fixed overnight at room temperature in 10% neutral-buffered formalin, followed by standard paraffin-embedding (Leica TP1020 Tissue Processor, Leica Biosystems, Wetzlar, Germany).

Genotyping

Mouse tails snips were digested in 500 µL DNA digestion buffer (50 mM Tris pH 8.0, 100 mM EDTA pH 8.0, 100 mM NaCl, 1% SDS) supplemented with 0.5 mg/mL proteinase K (Sigma-Aldrich) for 2 hours at 55°C in a thermal shaker (Thermo Fisher Scientific, MS, USA). Next, DNA was extracted following the phenol-chloroform protocol. 0.7 mL neutralized phenol/chloroform/iso-amylalcohol (25:24:1, Thermo Fisher Scientific) was added to each sample and mixed for 1hr. Afterwards samples were centrifuged (5 min., 14000 rpm) and 0.5 mL of the upper phase was transferred to a new tube. 1 mL of 100% ethanol at room temperature was added to each sample followed by centrifugation (5 min., 14000 rpm). The supernatant was carefully removed and 1 mL of 70% ethanol at -20°C was added, the tubes

were inverted several times and centrifuged (5 min., 14000 rpm). The supernatant was again carefully removed and the pellet was dried for 15 min. at room temperature. Finally, each pellet was resuspended in 150 µL Tris-EDTA (10mM Tris pH 8.0, 1 mM EDTA) and heated for 15 min. at 65°C.

DNA concentration was measured with a NanoDrop ND-1000 UV Visible Spectrophotometer (Thermo Fisher Scientific) and diluted with nuclease-free water to 2.5 ng DNA per µL. 2 µL of DNA sample was added to 10.5 µL PCR reaction mixture (3 µL nuclease-free H_2O, 6.25 µL 2x M-PCR OPTI Mix (Mouse Direct PCR Kit, Bimake, Houston, TX, USA), 0.62 µL 5% (v/v) DMSO and 0.31 µL of 20 µM forward and reverse primer (**Supplementary Table S16**). DNA amplification was done with a 2720 Thermal Cycler (Applied Biosystems, Thermo Fisher Scientific) with initial denaturation (5 min. at 94°C) followed by 35 cycles of denaturation (20 sec. at 94°C), annealing (30 sec. at 60°C), extension (30 sec. 72°C) and a final extension (5 min. at 72°C). PCR samples were run on a 1.5% agarose gel for 1hr at 120V.

Immunostaining

Paraffin-embedded pancreas and spleen sections were cut using a rotary microtome (HM340E, Thermo Fisher Scientific). Prior to immunostaining, slides were heated at 65°C for 60 min., followed by dewaxing in xylene (2 x 5 min.) and rehydration in 95% ethanol (2 x 2 min.) and rinsed for 5 min. under running distilled water. Choice of antigen-retrieval method depended on the antigen under study (**Supplementary Table S17**). Heat-mediated antigen-retrieval (HIER) was done in a pressure cooker (Retriever, Electron Microscopy Sciences, Hatfield, PA, USA) using 10 mM citrate pH 6.0, followed by 30 min. cool down at room temperature and 5 min. rinsing with running distilled water. For proteinase K-mediated antigen retrieval, sections were incubated for 15 min. with proteinase K (1 drop proteinase K (Dako, Agilent, Santa Clara, CA, USA) per 2.0 mL 0.05M Tris-HCl pH 7.7). To prevent non-specific binding, sections were incubated for 30 min. in Blocker Casein (Thermo Fisher Scientific) diluted 1:4 in PBST (PBS + 0.1% (v/v) Tween-20). Next, sections were incubated overnight at 4°C with primary antibody (**Supplementary Table S17**) diluted in PBST + 0.1% IgG-free BSA (Jackson Immunoresearch, Newmarket, UK). Next, slides were washed 2 x 5 min. in PBST and sections were incubated for 1 hour at room temperature with AlexaFluor or Cyanine-labelled secondary antibodies (Jackson Immunoresearch) diluted 1:500 in PBST. Biotinylated tomato Lectin was visualized with AlexaFluor 555-labelled streptavidin (Thermo Fisher Scientific). Nuclei were labelled with Hoechst 33342 at 4 ug/mL. After a final wash (2 x 5 min. in PBST), slides were mounted with aqueous mounting medium (Abcam, Cambridge, UK). Images were captured with an Olympus BX61 microscope (Olympus, Tokyo, Japan) equipped with an Orca r^2 camera (Hamamatsu Photonics, Hamamatsu, Japan) and SmartCapture3 (Digital Scientific UK, Cambridge, UK). Image analysis was done using Fiji (Schindelin et al. 2009).

Statistical analysis

A minimum of 2500 cells were counted for each data point. Results are presented as mean ± SEM. Data presentation and analysis were performed using GraphPad Prism 8.3 (GraphPad, San Diego, CA, USA). Two-tailed student t-test and non-parametric One-Way ANOVA were used to identify differences between groups and considered statistically significant if $p < 0.05$.

References

Alonso, Laura C et al. 2007. “Glucose Infusion in Mice: A New Model to Induce Beta-Cell Replication.” *Diabetes* **56**(7): 1792–1801.

Ashoor, Maryam F., Afra K. Bintouq, Martin K. Rutter, and Rayaz A. Malik. 2016. “Pancreatic Islet Cell Transplantation as a Treatment for Brittle Type 1 Diabetes: A Case Report and Review of the Literature.” *Journal of Taibah University Medical Sciences* **11**(4): 395–400.

Atkinson, M. A., and G. S. Eisenbarth. 2001. “Type 1 Diabetes: New Perspectives on Disease Pathogenesis and Treatment.” *The Lancet* **358**(9277): 221–29.

Bonhoeffer, Sebastian, Hiroshi Mohri, David Ho, and S Alan. 2020. “Quantification of Cell Turnover Kinetics Using 5-Bromo-2 ′ -Deoxyuridine 1.” *Journal of Immunology* **164**(10): 5049–54.

Bottino, Rita, Massimo Trucco, A. N. Balamurugan, and Thomas E. Starzl. 2002. “Pancreas and Islet Cell Transplantation.” *Bailliere’s Best Practice and Research in Clinical Gastroenterology* **16**(3): 457–74.

Brissova, Marcela et al. 2006. “Pancreatic Islet Production of Vascular Endothelial Growth Factor-A Is Essential for Islet Vascularization, Revascularization, and Function.” *Diabetes* **55**(11): 2974–85.

Brissova, Marcela et al. 2014. “Islet Microenvironment, Modulated by Vascular Endothelial Growth Factor-A Signaling, Promotes β Cell Regeneration.” *Cell Metabolism* **19**(3): 498–511.

Butler, A. E. et al. 2003. “Beta-Cell Deficit and Increased-Beta-Cell Apoptosis in Humans With Type 2 Diabetes.” *Diabetes* **52**(1): 102–10.

Butler, A. E. et al. 2010. “Adaptive Changes in Pancreatic Beta Cell Fractional Area and Beta Cell Turnover in Human Pregnancy.” *Diabetologia* **53**(10): 2167–76.

Chen, Hainan et al. 2011. “PDGF Signalling Controls Age-Dependent Proliferation in Pancreatic β-Cells.” *Nature* **478**(7369): 349–55.

Chera, Simona et al. 2014. “Diabetes Recovery by Age-Dependent Conversion of Pancreatic δ-Cells into Insulin Producers.” *Nature* **514**(7253): 503–7.

Corish, Pete, and Chris Tyler-Smith. 1999. “Attenuation of Green Fluorescent Protein Half-Life in Mammalian Cells.” *Protein Engineering* **12**(12): 1035–40.

D’Hoker, Joke et al. 2013. “Conditional Hypovascularization and Hypoxia in Islets Do Not Overtly Influence Adult B-Cell Mass or Function.” *Diabetes* **62**(12): 4165–73.

Dor, Yuval, Juliana Brown, Olga I Martinez, and Douglas A Melton. 2004. “Adult Pancreatic Beta-Cells Are Formed by Self-Duplication Rather than Stem-Cell Differentiation.” *Nature* **429**(6987): 41–46.

Eberhard, Daniel, and Eckhard Lammert. 2009. “The Pancreatic β-Cell in the Islet and Organ Community.” *Current Opinion in Genetics and Development* **19**(5): 469–75.

Georgia, Senta, and Anil Bhushan. 2004. “β Cell Replication Is the Primary Mechanism for Maintaining Postnatal β Cell Mass.” *Journal of Clinical Investigation* **114**(7): 963–68.

Geron, Erez, Sigalit Boura-Halfon, Eyal D. Schejter, and Ben Zion Shilo. 2015. “The Edges of Pancreatic Islet β Cells Constitute Adhesive and Signaling Microdomains.” *Cell Reports* **10**(3): 317–25.

Grün, Dominic et al. 2016. “De Novo Prediction of Stem Cell Identity Using Single-Cell Transcriptome Data.” *Cell Stem Cell* **19**(2): 266–77.

Guney, Michelle A. et al. 2011. “Connective Tissue Growth Factor Acts within Both Endothelial Cells and β Cells to Promote Proliferation of Developing β Cells.” *Proceedings of the National*

Academy of Sciences of the United States of America **108**(37): 15242–47.

Huo, Lili et al. 2016. "Life Expectancy of Type 1 Diabetic Patients during 1997–2010: A National Australian Registry-Based Cohort Study." *Diabetologia* **59**(6): 1177–85.

Lammert, E., O. Cleaver, and D. Melton. 2001. "Induction of Pancreatic Differentiation by Signals from Blood Vessels." *Science* **294**(5542): 564–67.

Lammert, E et al. 2003. "Role of VEGF-A in Vascularization of Pancreatic Islets." *Current Biology* **13**(12): 1070–74.

Lewandoski, M. 2001. "Conditional Control of Gene Expression in the Mouse." *Nature Reviews Genetics* **2**(10): 743–55.

Mazzetti, S. et al. 2004. "Lycopersicon Esculentum Lectin: An Effective and Versatile Endothelial Marker of Normal and Tumoral Blood Vessels in the Central Nervous System." *European journal of histochemistry : EJH* **48**(4): 423–28.

Meier, J et al. 2008. "Beta-Cell Replication Is the Primary Mechanism Subserving the Postnatal Expansion of Beta-Cell Mass in Humans." *Diabetes* **57**(6): 1584–94.

Muraro, Mauro J. et al. 2016. "A Single-Cell Transcriptome Atlas of the Human Pancreas." *Cell Systems* **3**(4): 385-394.e3.

Murtaugh, L Charles. 2007. "Pancreas and Beta-Cell Development : From the Actual to the Possible." *Development* **134**(3): 427–38.

Nikolova, Ganka et al. 2006. "The Vascular Basement Membrane: A Niche for Insulin Gene Expression and β Cell Proliferation." *Developmental Cell* **10**(3): 397–405.

Noble, Janelle A., and Ana M. Valdes. 2011. "Genetics of the HLA Region in the Prediction of Type 1 Diabetes." *Current Diabetes Reports* **11**(6): 533–42.

Papatheodorou, Konstantinos et al. 2016. "Complications of Diabetes 2016." *Journal of Diabetes Research* **2016**(6989453.).

Perl, Shira Y. et al. 2010. "Significant Human β-Cell Turnover Is Limited to the First Three Decades of Life as Determined by in Vivo Thymidine Analog Incorporation and Radiocarbon Dating." *Journal of Clinical Endocrinology and Metabolism* **95**(10): E234–39.

Polonsky, William H. 1999. *Diabetes Burnout: What to Do When You Can't Take It Anymore*. American Diabetes Association Inc.

Reers, Christina et al. 2009. "Impaired Islet Turnover in Human Donor Pancreata with Aging." *Eur J endocrinol.* **160**(2): 185–91.

Reneker, Lixing W., Huiyi Chen, and P. A. Overbeek. 2011. "Activation of Unfolded Protein Response in Transgenic Mouse Lenses." *Investigative Ophthalmology and Visual Science* **52**(5): 2100–2108.

Rewers, Marian, and Johnny Ludvigsson. 2016. "Environmental Risk Factors for Type 1 Diabetes." *The Lancet* **387**(10035): 2340–48.

Riley, Kimberly G. et al. 2015. "Connective Tissue Growth Factor Modulates Adult β-Cell Maturity and Proliferation to Promote β-Cell Regeneration in Mice." *Diabetes* **64**(4): 1284–98.

Roh, Ji Yeol et al. 2013. "Modification of Enhanced Green Fluorescent Protein for Secretion out of Cells." *Biotechnology and Bioprocess Engineering* **18**(6): 1135–41.

Ryan, Edmond A et al. 2002. "Successful Islet Transplantation: Continued Insulin Reserve Provides Long-Term Glycemic Control." *Diabetes* **51**(7): 2148–57.

Ryding, A. D.S., M. G.F. Sharp, and J. J. Mullins. 2001. "Conditional Transgenic Technologies." *Journal*

of Endocrinology **171**(1): 1–14.

Scaglia, L, C J Cahill, D T Finegood, and S Bonner-Weir. 1997. “Apoptosis Participates in the Remodeling of the Endocrine Pancreas in the Neonatal Rat.” *Endocrinology* **138**(4): 1736-1741.

Schindelin, Johannes et al. 2009. “Fiji - an Open Platform for Biological Image Analysis.” *Nature Methods* **9**(7): 676–82.

Sharma, Rohit B et al. 2015. “Insulin Demand Regulates Beta Cell Number via the Unfolded Protein Response.” *J Clin Invest* **125**(10): 3831–46.

Staels, Willem et al. 2017. “Conditional Islet Hypovascularisation Does Not Preclude Beta Cell Expansion during Pregnancy in Mice.” *Diabetologia* **60**(6): 1051–56.

Strowitzki, M. J., E. P. Cummins, and C. T. Taylor. 2019. “Protein Hydroxylation by Hypoxia-Inducible Factor (HIF) Hydroxylases: Unique or Ubiquitous?” *Cells* **8**(5): 384.

Szabat, Marta et al. 2016. “Reduced Insulin Production Relieves Endoplasmic Reticulum Stress and Induces β Cell Proliferation.” *Cell Metabolism* **23**(1): 179–93.

Thorel, Fabrizio et al. 2010. “Conversion of Adult Pancreatic α Alpha-Cells to Beta-Cells after Extreme Beta-Cell Loss.” *Nature* **464**(7292): 1149–54.

Supplementary information

Pancreatic intra-islet vessel ablation and regeneration as a model for promoting active beta and delta cell cycling

Supplementary tables

Supplementary table S1: Statistical analysis of sFLT1 expression in dTg no DOX, dTg +DOX WD 1d, 4d and 7d mice.

sFLT1 expression					
Descriptive statistics					
Groups	no DOX	+DOX, WD 1d	+DOX, WD 4d	+DOX, WD 7d	
Number of values	4	3	2	9	
Mean	2,717	42,58	34,56	19,83	
Std. Deviation	1,373	1,584	9,202	5,932	
Std. Error of Mean	0,6867	0,9144	6,507	1,977	
Test for normal distribution					
Shapiro-Wilk test					
W	0,8704	0,7642	0,843		
P value	0,2991	0,0317	0,0623		
Passed normality test (alpha=0.05)?	Yes	No	Yes		
P value summary	ns	*	ns		
Ordinary One-Way ANOVA: multiple comparisons					
Number of families	1				
Number of comparisons per family	3				
Alpha	0,05				
Tukey's multiple comparisons test	Mean Diff,	95,00% CI of diff,	Significant?	Summary	Adjusted P Value
no DOX vs. +DOX, WD 1d	-39,86	-49,43 to -30,30	Yes	****	<0,0001
no DOX vs. +DOX, WD 7d	-17,12	-24,64 to -9,595	Yes	***	0,0001
+DOX, WD 1d vs. +DOX, WD 7d	22,75	14,40 to 31,09	Yes	****	<0,0001

Supplementary table S2: Statistical analysis of islet vessel area over islet area in dTg no DOX, dTg +DOX WD 1d, 4d and 7d mice.

Vessel density					
Descriptive statistics					
Groups	no DOX	+DOX, WD 1d	+DOX, WD 4d	+DOX, WD 7d	
Number of values	5	3	2	8	
Mean	7,827	1,698	1,418	2,273	
Std. Deviation	1,505	0,24	0,01042	0,5073	
Std. Error of Mean	0,6732	0,1386	0,007371	0,1793	
Test for normal distribution					
Shapiro-Wilk test					
W	0,9398	0,9017	0,8874		
P value	0,6644	0,3908	0,2215		
Passed normality test (alpha=0.05)?	Yes	Yes	Yes		
P value summary	ns	ns	ns		
Ordinary One-way ANOVA: multiple comparisons					
Number of families	1				
Number of comparisons per family	3				
Alpha	0,05				
Tukey's multiple comparisons test	Mean Diff,	95,00% CI of diff,	Significant?	Summary	Adjusted P Value
no DOX vs. +DOX, WD 1d	6,129	4,357 to 7,902	Yes	****	<0,0001
no DOX vs. +DOX, WD 7d	5,554	4,171 to 6,938	Yes	****	<0,0001
+DOX, WD 1d vs. +DOX, WD 7d	-0,5752	-2,218 to 1,068	No	ns	0,6351

Supplementary Table S3: Statistical analysis of 2hrs FG in dTg +DOX mice at start, day 7 and day 14 of DOX administration.

2hrs fasting glycaemia dTg +DOX during DOX administration					
Descriptive statistics					
Groups	Day 0	Day 7	Day 14		
Number of values	20	20	20		
Mean	160,6	184,8	198,2		
Std. Deviation	34,35	39,27	42,27		
Std. Error of Mean	7,682	8,782	9,452		
Test for normal distribution					
Anderson-Darling test					
A2*	0,5609	0,6105	0,3489		
P value	0,1277	0,0969	0,4394		
Passed normality test (alpha=0.05)?	Yes	Yes	Yes		
P value summary	ns	ns	ns		
Ordinary One-way ANOVA: multiple comparisons					
Number of families	1				
Number of comparisons per family	3				
Alpha	0,05				
Tukey's multiple comparisons test	Mean Diff,	95,00% CI of diff,	Significant?	Summary	Adjusted P Value
Day 0 vs. Day 7	-24,25	-53,75 to 5,253	No	ns	0,1269
Day 0 vs. Day 14	-37,65	-67,15 to -8,147	Yes	**	0,009
Day 7 vs. Day 14	-13,4	-42,90 to 16,10	No	ns	0,5223

Supplementary Table S4: Statistical analysis of 2hrs FG in dTg no DOX, sTg +DOX and dTg +DOX mice at day 0 (start of DOX administration).

2hrs fasting glycaemia day 0					
Descriptive statistics					
Groups	dTg no DOX	sTg +DOX	dTg +DOX		
Number of values	8	15	20		
Mean	167,1	157,7	160,6		
Std. Deviation	51,97	34,13	34,35		
Std. Error of Mean	18,37	8,812	7,682		
Test for normal distribution					
Anderson-Darling test					
A2*	0,2471	0,87	0,5609		
P value	0,6478	0,0192	0,1277		
Passed normality test (alpha=0.05)?	Yes	No	Yes		
P value summary	ns	*	ns		
Kruskal-Wallis test: Multiple comparisons					
Number of families	1				
Number of comparisons per family	3				
Alpha	0,05				
Dunn's multiple comparisons test	Mean rank diff,	Significant?	Summary	Adjusted P Value	
dTg no DOX vs. sTg +DOX	2,483	No	ns	>0,9999	
dTg no DOX vs. dTg +DOX	1,9	No	ns	>0,9999	
sTg +DOX vs. dTg +DOX	-0,5833	No	ns	>0,9999	

Supplementary Table S5: Statistical analysis of 2hrs FG in dTg no DOX, sTg +DOX and dTg +DOX mice at day 7 during DOX administration.

2hrs fasting glycaemia day 7					
Descriptive statistics					
Groups	dTg no DOX	sTg +DOX	dTg +DOX		
Number of values	8	15	20		
Mean	184,9	154,7	184,8		
Std. Deviation	49,2	36,94	39,27		
Std. Error of Mean	17,4	9,538	8,782		
Test for normal distribution					
Anderson-Darling test					
A2*	0,3987	0,3663	0,6105		
P value	0,2759	0,3861	0,0969		
Passed normality test (alpha=0.05)?	Yes	Yes	Yes		
P value summary	ns	ns	ns		
Ordinary One-way ANOVA: multiple comparisons					
Number of families	1				
Number of comparisons per family	3				
Alpha	0,05				
Tukey's multiple comparisons test	Mean Diff,	95,00% CI of diff,	Significant?	Summary	Adjusted P Value
dTg no DOX vs. sTg +DOX	30,21	-12,86 to 73,28	No	ns	0,2151
dTg no DOX vs. dTg +DOX	0,075	-41,08 to 41,23	No	ns	>0,9999
sTg +DOX vs. dTg +DOX	-30,13	-63,74 to 3,470	No	ns	0,0865

Supplementary Table S6: Statistical analysis of 2hrs FG in dTg no DOX, sTg +DOX and dTg +DOX mice at day 14 during DOX administration.

2hrs fasting glycaemia day 14					
Descriptive statistics					
Groups	dTg no DOX	sTg +DOX	dTg +DOX		
Number of values	8	15	20		
Mean	165,3	143,2	198,2		
Std. Deviation	52,91	27,41	42,27		
Std. Error of Mean	18,71	7,078	9,452		
Test for normal distribution					
Anderson-Darling test					
A2*	0,6245	0,3403	0,3489		
P value	0,0658	0,447	0,4394		
Passed normality test (alpha=0.05)?	Yes	Yes	Yes		
P value summary	ns	ns	ns		
Ordinary One-way ANOVA: multiple comparisons					
Number of families	1				
Number of comparisons per family	3				
Alpha	0,05				
Tukey's multiple comparisons test	Mean Diff,	95,00% CI of diff,	Significant?	Summary	Adjusted P Value
dTg no DOX vs. sTg +DOX	22,05	-20,59 to 64,69	No	ns	0,4266
dTg no DOX vs. dTg +DOX	-32,95	-73,70 to 7,799	No	ns	0,1334
sTg +DOX vs. dTg +DOX	-55	-88,27 to -21,73	Yes	***	0,0007

Supplementary Table S7: Statistical analysis of 2hrs FG in dTg no DOX, sTg +DOX and dTg +DOX mice at day 21 (WD 7d of DOX).

2hrs fasting glycaemia day 21					
Descriptive statistics					
Groups	dTg no DOX	sTg +DOX	dTg +DOX		
Number of values	8	11	14		
Mean	137,8	137,1	155,6		
Std. Deviation	14,04	12,03	19,28		
Std. Error of Mean	4,963	3,627	5,152		
Test for normal distribution					
Anderson-Darling test					
A2*	0,1464	0,278	0,4135		
P value	0,9411	0,5765	0,2911		
Passed normality test (alpha=0.05)?	Yes	Yes	Yes		
P value summary	ns	ns	ns		
Ordinary One-way ANOVA: multiple comparisons					
Number of families	1				
Number of comparisons per family	3				
Alpha	0,05				
Tukey's multiple comparisons test	Mean Diff,	95,00% CI of diff,	Significant?	Summary	Adjusted P Value
dTg no DOX vs. sTg +DOX	0,6591	-17,64 to 18,96	No	ns	0,9957
dTg no DOX vs. dTg +DOX	-17,89	-35,35 to -0,4365	Yes	*	0,0437
sTg +DOX vs. dTg +DOX	-18,55	-34,42 to -2,683	Yes	*	0,0192

Supplementary Table S8: Statistical analysis of active beta cell cycling in dTg no DOX, sTg +DOX and dTg +DOX WD 7d mice following recovery from intra-islet vessel ablation.

Active beta cell cycling					
Descriptive statistics					
Groups	dTg no DOX	sTg +DOX WD 7d	dTg +DOX WD 7d		
Number of values	8	6	10		
Mean	2,672	3,583	6,516		
Std. Deviation	0,7001	1,427	2,149		
Std. Error of Mean	0,2475	0,5827	0,6796		
Test for normal distribution					
Shapiro-Wilk test					
W	0,9505	0,963	0,9493		
P value	0,7167	0,8425	0,6606		
Passed normality test (alpha=0.05)?	Yes	Yes	Yes		
P value summary	ns	ns	ns		
Ordinary One-way ANOVA: multiple comparisons					
Number of families	1				
Number of comparisons per family	3				
Alpha	0,05				
Tukey's multiple comparisons test	Mean Diff,	95,00% CI of diff,	Significant?	Summary	Adjusted P Value
dTg no DOX vs. sTg +DOX WD 7d	-0,9111	-3,118 to 1,296	No	ns	0,5602
dTg no DOX vs. dTg +DOX WD 7d	-3,844	-5,782 to -1,906	Yes	***	0,0002
sTg +DOX WD 7d vs. dTg +DOX WD	-2,933	-5,043 to -0,8232	Yes	**	0,0057

Supplementary Table S9: Statistical analysis of fold change in active beta cell cycling in dTg no DOX, sTg +DOX and dTg +DOX WD 7d mice following recovery from intra-islet vessel ablation.

Fold change Active beta cell cycling					
Descriptive statistics					
Groups	dTg no DOX	sTg +DOX WD 7d	dTg +DOX WD 7d		
Number of values	8	6	10		
Mean	1	1,341	2,439		
Std. Deviation	0,262	0,5342	0,805		
Std. Error of Mean	0,09263	0,2181	0,2546		
Test for normal distribution					
Shapiro-Wilk test					
W	0,9505	0,963	0,9493		
P value	0,7167	0,8425	0,6602		
Passed normality test (alpha=0.05)?	Yes	Yes	Yes		
P value summary	ns	ns	ns		
Ordinary One-way ANOVA: multiple comparisons					
Number of families	1				
Number of comparisons per family	3				
Alpha	0,05				
Tukey's multiple comparisons test	Mean Diff,	95,00% CI of diff,	Significant?	Summary	Adjusted P Value
dTg no DOX vs. sTg +DOX WD 7d	-0,341	-1,167 to 0,4854	No	ns	0,5606
dTg no DOX vs. dTg +DOX WD 7d	-1,439	-2,165 to -0,7131	Yes	***	0,0002
sTg +DOX WD 7d vs. dTg +DOX WD	-1,098	-1,888 to -0,3077	Yes	**	0,0058

Supplementary Table S10: Statistical analysis of active delta cell cycling in dTg no DOX, sTg +DOX and dTg +DOX WD 7d following recovery from intra-islet vessel ablation.

Active delta cell cycling					
Descriptive statistics					
Groups	dTg no DOX	sTg +DOX WD 7d	dTg +DOX WD 7d		
Number of values	6	8	14		
Mean	3,332	3,476	6,4		
Std. Deviation	0,5308	1,183	1,977		
Std. Error of Mean	0,2167	0,4184	0,5284		
Test for normal distribution					
Shapiro-Wilk test					
W	0,9036	0,7582	0,9211		
P value	0,3958	0,0101	0,2283		
Passed normality test (alpha=0.05)?	Yes	No	Yes		
P value summary	ns	*	ns		
Kruskal-Wallis test: Multiple comparisons					
Number of families	1				
Number of comparisons per family	3				
Alpha	0,05				
Dunn's multiple comparisons test	Mean rank diff,	Significant?	Summary	Adjusted P Value	
dTg no DOX vs. sTg +DOX WD 7d	-0,1667	No	ns	>0,9999	
dTg no DOX vs. dTg +DOX WD 7d	-12,24	Yes	**	0,0069	
sTg +DOX WD 7d vs. dTg +DOX WD	-12,07	Yes	**	0,0028	

Supplementary Table S11: Statistical analysis of fold change in active delta cell cycling in dTg no DOX, sTg +DOX and dTg +DOX WD 7d following recovery from intra-islet vessel ablation.

Fold change active delta cell cycling					
Descriptive statistics					
Groups	dTg no DOX	sTg +DOX WD 7d	dTg +DOX WD 7d		
Number of values	6	8	14		
Mean	1	1,043	1,92		
Std. Deviation	0,1593	0,3551	0,5934		
Std. Error of Mean	0,06503	0,1255	0,1586		
Test for normal distribution					
Shapiro-Wilk test					
W	0,9036	0,7582	0,9211		
P value	0,3958	0,0101	0,2283		
Passed normality test (alpha=0.05)?	Yes	No	Yes		
P value summary	ns	*	ns		
Kruskal-Wallis test: Multiple comparisons					
Number of families	1				
Number of comparisons per family	3				
Alpha	0,05				
Dunn's multiple comparisons test	Mean rank diff,	Significant?	Summary	Adjusted P Value	
dTg no DOX vs. sTg +DOX WD 7d	-0,1667	No	ns	>0,9999	
dTg no DOX vs. dTg +DOX WD 7d	-12,24	Yes	**	0,0069	
sTg +DOX WD 7d vs. dTg +DOX WD	-12,07	Yes	**	0,0028	

Supplementary Table S12: Statistical analysis of 2hrs FG in RIP-rtTA;TetO-GFP dTg +DOX mice at day 0 and day 14 of DOX administration.

2hrs FG all groups at day 14 DOX administration		
Descriptive statistics		
Groups	Day 0	Day 14
Number of values	11	12
Mean	138,3	150,7
Std. Deviation	13,84	20,08
Std. Error of Mean	4,174	5,796
Test for normal distribution		
Anderson-Darling test		
A2*	0,3866	0,2031
P value	0,3251	0,8381
Passed normality test (alpha=0.05)?	Yes	Yes
P value summary	ns	ns
Unpaired t test		
Column B	Day 14	
vs.	vs,	
Column A	Day 0	
Unpaired t test		
P value	0,1025	
P value summary	ns	
Significantly different (P < 0.05)?	No	
One- or two-tailed P value?	Two-tailed	
t, df	t=1,707, df=21	

Supplementary Table S13: Statistical analysis of 2hrs FG in RIP-rtTA;tetO-GFP dTg no DOX and dTg +DOX mice at 14 days of DOX administration.

2hrs FG all groups at day 14 DOX administration		
Descriptive statistics		
Groups	dTg no DOX	dTg +DOX
Number of values	7	12
Mean	145	150,7
Std. Deviation	12,5	20,08
Std. Error of Mean	4,726	5,796
Test for normal distribution		
Shapiro-Wilk test		
W	0,932	0,9759
P value	0,5676	0,9618
Passed normality test (alpha=0.05)?	Yes	Yes
P value summary	ns	ns
Unpaired t test		
Column B	dTg +DOX	
vs.	vs,	
Column A	dTg no DOX	
Unpaired t test		
P value	0,5117	
P value summary	ns	
Significantly different (P < 0.05)?	No	
One- or two-tailed P value?	Two-tailed	
t, df	t=0,6702, df=17	

Supplementary Table 14: Statistical analysis of GFP expression in dTg 14d +DOX and dTg 14d +DOX WD 7d mice.

GFP expression		
Descriptive statistics		
Groups	dTg 14d +DOX	dTg 14d +DOX WD 7d
Number of values	3	5
Mean	29,61	14,87
Std. Deviation	2,809	4,572
Std. Error of Mean	1,622	2,045
Test for normal distribution		
Shapiro-Wilk test		
W	0,9867	0,9547
P value	0,7797	0,7708
Passed normality test (alpha=0.05)?	Yes	Yes
P value summary	ns	ns
Unpaired t test		
Column B	dTg 14d +DOX WD 7d	
vs.	vs,	
Column A	dTg 14d +DOX	
Unpaired t test		
P value	0,0026	
P value summary	**	
Significantly different (P < 0.05)?	Yes	
One- or two-tailed P value?	Two-tailed	
t, df	t=4,957, df=6	

Supplementary Table 15: Statistical analysis of active beta cell cycling in RIP-rtTA;tetO-GFP dTg no DOX and dTg +DOX WD 7d mice.

Active beta cell cycling		
Descriptive statistics		
Groups	dTg no DOX	dTg +DOX WD 7d
Number of values	5	9
Mean	4,714	7,325
Std. Deviation	2,811	1,895
Std. Error of Mean	1,257	0,6317
Test for normal distribution		
Shapiro-Wilk test		
W	0,8088	0,8653
P value	0,0955	0,1095
Passed normality test (alpha=0.05)?	Yes	Yes
P value summary	ns	ns
Unpaired t test		
Column B	dTg +DOX WD 7d	
vs.	vs,	
Column A	dTg no DOX	
Unpaired t test		
P value	0,0588	
P value summary	ns	
Significantly different (P < 0.05)?	No	
One- or two-tailed P value?	Two-tailed	
t, df	t=2,088, df=12	

Supplementary Table 16: Primer sequences used for genotyping

Target	Forward primer	Reverse primer
RIPrtTA	5'-TAGATGTGCTTTACTAAGTCATCGCG-3'	5'- GAGATCGAGCGGGCCCTCGATGGTAG-3'
tetO-sFLT1	5'-CGACTCACTATAGGGAGACCC-3'	5'-TGGCCTGCTTGCATGATGTGCTGG-3'
tetO-GFP	5'-GGTAAAACTTTGTGACAAGGACCA-3'	5'-GGACATATGGGAGGGCAAATC-3' 5'-GCAACTTCTGCGCTCAACAA-3'

Supplementary Table S17: Primary antibodies used for immunostaining

Target	Host	Antigen retrieval	Dilution	Source
BrdU	Mouse	HIER	1:50	Dako
FLT1/VEGF-R1	Rabbit	HIER	1:50	Santa Cruz
GFP	Goat	HIER	1:400	Abcam
Insulin	Guinea pig	HIER	1:50	DRC, VUB
NKX6.1	Goat	HIER	1:5000	R&D Systems
Somatostatin	Rat	HIER	1:100	Abcam